Extensional rheology of active suspensions

David Saintillan*
Department of Mechanical Science and Engineering, University of Illinois at Urbana–Champaign, Urbana, Illinois 61801, USA
(Received 1 December 2009; published 10 May 2010)

A simple model is presented for the effective extensional rheology of a dilute suspension of active particles, such as self-propelled microswimmers, extending previous classical studies on suspensions of passive rodlike particles. Neglecting particle-particle hydrodynamic interactions, we characterize the configuration of the suspension by an orientation distribution, which satisfies a Fokker-Planck equation including the effects of an external flow field and of rotary diffusion. Knowledge of this orientation distribution then allows the determination of the particle extra stress as a configurational average of the force dipoles exerted by the particles on the fluid, which involve contributions from the imposed flow, rotary diffusion, and the permanent dipoles resulting from activity. Analytical expressions are obtained for the stress tensor in uniaxial extensional and compressional flows, as well as in planar extensional flow. In all types of flows, the effective viscosity is found to increase as a result of activity in suspensions of head-actuated swimmers (pullers) and to decrease in suspensions of tail-actuated swimmers (pushers). In the latter case, a negative particle viscosity is found to occur in weak flows. In planar extensional flow, we also characterize normal stresses, which are enhanced by activity in suspensions of pullers but reduced in suspensions of pushers. Finally, an energetic interpretation of the seemingly unphysical decrease in viscosity predicted in suspensions of pushers is proposed, where the decrease is explained as a consequence of the active power input generated by the swimming particles and is shown not to be directly related to viscous dissipative processes.

DOI: 10.1103/PhysRevE.81.056307 PACS number(s): 47.63.Gd, 83.10.−y, 47.57.−s, 47.50.−d

I. INTRODUCTION

An active suspension denotes a suspension of particles that are motile and inject mechanical energy into the suspending fluid, usually as a result of self-propulsion. Typical examples include suspensions of living microorganisms and swimming cells (e.g., bacteria, algae, and sperm) [1,2], as well as suspensions of artificial microswimmers [3–7]. These systems have been the center of much attention recently, owing to their relevance in ecology [8,9], pathology [10], as well as various technological applications [11,12]. They are also interesting from a more fundamental perspective as their dynamics and properties differ quite uniquely from those of passive particle suspensions.

The mechanisms by which living microorganisms are able to swim at small scales are varied [1,13] and include appendages such as flagella [2,14,15], ciliated surfaces [2], body deformations [16], and actin-tail polymerization [17,18]. Artificial swimmers also use other mechanisms, including chemical reactions [3–5] and actuation by an external magnetic field [6,7]. While these mechanisms can seem very different, they also share universal features. In all cases, the self-propelled particle exerts a propulsive force on the surrounding fluid, which may be unsteady but has a nonzero mean in the direction of swimming. Because the overall particle is force free (if gravity can be neglected), this propulsive force must be balanced exactly by the viscous drag on the body as it moves through the fluid. To leading order, the net forcing exerted by the particle on the fluid is therefore a force dipole, the magnitude of which will be denoted by σ_0. While σ_0 is likely to fluctuate with time for most common swimming mechanisms, possibly resulting in interesting phenomena [19], we assume here that it remains constant, which is a valid approximation if the macroscopic time scales of interest are much larger than the time scale for microswimming actuation. The sign and magnitude of σ_0 both depend on the precise propulsion mechanism: in particular, a tail-actuated swimmer or pusher, such as most swimming bacteria including *Escherichia Coli* and *Bacillus Subtilis*, will result in $\sigma_0<0$, whereas head-actuated swimmers or pullers, such as the alga *Chlamydomonas Reinhardtii*, will result in $\sigma_0>0$. This representation of a self-propelled particle as an effective force dipole exerted on the fluid is the basis for many models of swimming microorganisms [20–30], as well as for the present work.

One direct consequence of this effective dipole is the creation of a disturbance flow in the fluid, which can result in hydrodynamic interactions in suspensions of many particles. These interactions have been the subject of many theoretical [20,24–26,28–30] and computational [21–23,27,31–33] studies, and have been identified as the origin of the complex correlated motions, chaotic flows, and pattern formation that have been reported in experiments on active suspensions [34–39]. In addition to resulting in hydrodynamic interactions, the force dipoles exerted by the particles are also expected to modify the effective rheology of their suspensions. This observation is motivated by the classical Kirkwood theory [40,41] or by Batchelor's similar theory for particulate suspensions [42,43], which expresses the effective stress induced by a distribution of particles as a volume average of the force dipoles on the particles.

Very few experimental studies have tried to measure the effective rheology of microswimmer suspensions and yet strikingly demonstrate the nontrivial effects of activity. In recent work, Sokolov and Aranson [44] estimated the effective viscosity of a suspension of swimming *Bacillus Subtilis*,

*dstn@illinois.edu

which is a pusher, by measuring the viscous torque on a rotating magnetic particle immersed in a suspension film: they observed a strong decrease in the effective viscosity, by up to a factor of 7, and this decrease was found to strongly correlate with the swimming speed of the bacteria, which is a measure of activity. Rafaï *et al.* [45] also recently considered suspensions of swimming *Chlamydomonas Reinhardtii*, a puller alga, and reported a significant increase in viscosity in suspensions of swimming cells with respect to suspensions of dead cells at the same volume fraction. Note, however, that at the high volume fractions considered in their study, interactions between flagella may have had an effect on the effective suspension viscosity. While the conclusions of these two studies appear to be contradictory, we will see below that they are both valid and differ as a result of the distinct mechanisms for swimming (pusher vs puller).

A few theoretical and computational models have also been developed to predict the effective rheology of active suspensions. Hatwalne *et al.* [46] extended previous phenomenological models for the linear viscoelasticity of liquid crystals to account for active stresses (in the spirit of [20]), and predicted that activity should result in an effective increase in viscosity in suspensions of puller particles, but in a decrease in suspensions of pushers. More recently, Ishikawa and Pedley [47] performed Stokesian dynamics simulations of spherical swimmers that propel themselves by means of a prescribed surface slip velocity; however, they found no change in viscosity in the dilute limit (first correction in volume fraction) in the case of non-bottom-heavy particles, a likely consequence of the spherical shape of the particles, which results in an isotropic orientation distribution. Indeed, Haines *et al.* [48] developed a simple two-dimensional model and demonstrated the importance of the particle orientation distribution on the rheology: by assuming an *ad hoc* anisotropic distribution, they were able to predict a decrease in viscosity for pushers even for isotropic particles. More recently, they extended their model to three dimensions and developed a method of determination of the orientation distribution using asymptotic and numerical solutions of a Fokker-Planck equation, and obtained qualitatively similar results for the effective viscosity [49]. However, none of the aforementioned studies considered normal stresses.

In a recent paper, we developed a simple kinetic model for the effective rheology of a dilute active suspension in shear flow [50]. The model, which shares similarities with [49], extended classic theories for passive rod suspensions [51,52,54] and is based on a numerical solution of a conservation equation for the particle orientation distribution, which is then used to determine the particle extra stress using Batchelor's theory [42,43]. By adding an extra term accounting for the permanent force dipoles resulting from swimming, the effects of activity were investigated. We confirmed results from previous studies showing that the effective shear viscosity should increase in suspensions of pullers but decrease in suspensions of pushers, resulting in a negative particle viscosity in weak flows. We also estimated normal stresses and found that they are enhanced in suspensions of pullers, but change sign in suspensions of pushers.

In the present work, we extend the model of [50] to other common flow types, and specifically to irrotational flows. This work also directly extends previous classical studies on suspensions of passive rods [53,54] to account for activity. One significant simplification compared to the previous study of [50] on the effective rheology in shear flow is that the particle orientation distributions in irrotational flows can be determined exactly [54], yielding analytical expressions for the effective viscosity and normal stresses in the suspensions. The basic model for the particle orientation distribution and effective stress calculation is presented in Sec. II. It is then applied to uniaxial extensional and compressional flows in Sec. III, and to planar extensional flow in Sec. IV. For all flow types, results on the effective viscosity are presented, showing an increase in suspensions of pullers and a decrease in suspensions of pushers, in agreement with previous models and experiments; normal stresses are also analyzed in planar extensional flow. The origin of the seemingly unphysical negative particle viscosity that can be observed in pusher suspensions is further discussed in Sec. V, where an energy balance explains it as a consequence of the active power input resulting from activity, which is not a dissipative process. We conclude in Sec. VI.

II. BASIC THEORY

We consider a suspension of active particles such as self-propelled microswimmers of characteristic size l placed in an imposed linear straining flow with velocity field $\mathbf{u}(\mathbf{x})=\mathbf{x}\cdot\mathbf{E}$, where $\mathbf{E}$ denotes the rate-of-strain tensor and is a constant symmetric and traceless second-order tensor. If the suspension is dilute, particle-particle hydrodynamic interactions can be neglected, and we may assume that the suspension is spatially homogeneous. In this case, the configuration of the suspension is entirely determined by an orientation distribution $\Psi(\mathbf{p},t)$, where $\mathbf{p}$ denotes the particle director, which is a unit vector defining the particle orientation and swimming direction. The orientation distribution satisfies a Fokker-Planck equation [41],

$$\frac{\partial\Psi}{\partial t}+\boldsymbol{\nabla}_{\mathbf{p}}\cdot(\dot{\mathbf{p}}\Psi)-d\nabla_{\mathbf{p}}^2\Psi=0, \tag{1}$$

where $\boldsymbol{\nabla}_{\mathbf{p}}$ denotes the gradient operator on the surface of the unit sphere S,

$$\boldsymbol{\nabla}_{\mathbf{p}}\equiv(\mathbf{I}-\mathbf{pp})\cdot\frac{\partial}{\partial\mathbf{p}}, \tag{2}$$

and where $\Psi(\mathbf{p},t)$ is normalized by

$$\int_S\Psi(\mathbf{p},t)d\mathbf{p}=1. \tag{3}$$

In the following, we consider the steady-state case where Eq. (1) reduces to

$$\boldsymbol{\nabla}_{\mathbf{p}}\cdot(\dot{\mathbf{p}}\Psi-d\boldsymbol{\nabla}_{\mathbf{p}}\Psi)=0. \tag{4}$$

In Eq. (4), the first term models the effect of the external flow on the orientational dynamics of the particles and involves the angular velocity $\dot{\mathbf{p}}$ resulting from the flow. It is modeled by Jeffery's equation [55,56], which for an irrotational flow simplifies to

$$\dot{\mathbf{p}} = \beta(\mathbf{I} - \mathbf{pp}) \cdot \mathbf{E} \cdot \mathbf{p}, \tag{5}$$

where $\beta \in [-1,1]$ is a dimensionless parameter characterizing the particle shape, which is positive for prolate particles such as most biological or artificial microswimmers. Note also that $\beta \approx 1$ for a slender body.

The second term in Eq. (4) captures rotary diffusion of the particles, with constant diffusivity d. Rotary diffusion may arise as a result of Brownian fluctuations in suspensions of colloidal particles, such as some types of artificial microswimmers. While Brownian motion is typically negligible in suspensions of microorganisms, diffusion is still expected to occur in these systems as a result of hydrodynamic fluctuations, even in the dilute limit [31]. Here, we also use it as a simplified model for bacterial tumbling: while tumbling is not rigorously a diffusive process and is more accurately modeled by a Poisson process in orientation space [28,58], we demonstrated in a previous study [50] that its effects on the steady-state orientation distribution in the absence of interactions are qualitatively the same as those of rotary diffusion. In this work, we consider the case of slender particles of length l and inverse aspect ratio ϵ, for which the rotary diffusivity can be estimated based on slender-body theory as [41,57]

$$d = \frac{3kT \ln(2/\epsilon)}{\pi \mu l^3}. \tag{6}$$

In this expression kT denotes the thermal energy of the fluid in the case of a Brownian suspension or may be viewed as an effective thermal energy if d is used to model hydrodynamic diffusion or tumbling. Note that in the absence of Brownian motion, the system is not in thermal equilibrium, so that Eq. (6) is simply a convenient definition of an effective kT with no specific claim of thermodynamic relevance.

While Eq. (4) can only be solved numerically or asymptotically for an arbitrary linear flow, including a shear flow [50,59,60], Brenner and Condiff [53] showed that an analytical solution can be obtained in the case of irrotational linear flows such as the ones considered in this study. Indeed, using the symmetry of the tensor $\mathbf{E}$, Eq. (5) can be rewritten as

$$\dot{\mathbf{p}} = \frac{\beta}{2} \nabla_{\mathbf{p}} (\mathbf{pp}:\mathbf{E}). \tag{7}$$

This allows us to rewrite the steady-state Fokker-Planck equation (4) in the form

$$\nabla_{\mathbf{p}} \cdot \left[\Psi \nabla_{\mathbf{p}} \left(\frac{\beta}{2} \mathbf{pp}:\mathbf{E} - d \ln \Psi \right) \right] = 0. \tag{8}$$

A solution for $\Psi(\mathbf{p})$ is then easily obtained by setting the flux term to zero, yielding

$$\Psi(\mathbf{p}) = \frac{1}{K} \exp\left(\frac{\beta}{2d} \mathbf{pp}:\mathbf{E} \right), \tag{9}$$

where the normalization constant K is determined from Eq. (3) as

$$K = \int_S \exp\left(\frac{\beta}{2d} \mathbf{pp}:\mathbf{E} \right) d\mathbf{p}. \tag{10}$$

Once $\Psi(\mathbf{p})$ is known from Eq. (9), it can be used to evaluate the effective stress tensor in the suspension. Specifically, the total stress $\boldsymbol{\Sigma}$ is decomposed as the sum of the Newtonian stress and of a particle extra stress,

$$\boldsymbol{\Sigma} = -q\mathbf{I} + 2\mu\mathbf{E} + \boldsymbol{\Sigma}^p, \tag{11}$$

where q denotes the pressure and μ is the viscosity of the suspending fluid. In the dilute regime, the particle extra stress $\boldsymbol{\Sigma}^p$ is obtained as a configurational average of the force dipole $\mathbf{S}(\mathbf{p})$ exerted by a particle on the fluid,

$$\boldsymbol{\Sigma}^p = n\langle \mathbf{S}(\mathbf{p}) \rangle, \tag{12}$$

where n is the mean number density of the suspension and $\langle \cdot \rangle$ denotes the configurational average,

$$\langle \cdot \rangle = \int_S \cdot \Psi(\mathbf{p}) d\mathbf{p}. \tag{13}$$

In the case of interest, the dipole $\mathbf{S}(\mathbf{p})$ arises from several contributions, including resistance to stretching under the external flow, Brownian torques, and the permanent dipole due to self-propulsion [50]. The first two contributions, due to the external flow and to Brownian torques, were calculated previously as [51,52]

$$\mathbf{S}^f(\mathbf{p}) = A(\mathbf{pp}:\mathbf{E}) \left[\mathbf{pp} - \frac{\mathbf{I}}{3} \right], \tag{14}$$

$$\mathbf{S}^b(\mathbf{p}) = 3kT \left[\mathbf{pp} - \frac{\mathbf{I}}{3} \right]. \tag{15}$$

In Eq. (14), A is a constant depending on the particle shape; for a slender particle, it can be obtained from slender-body theory as $A = \pi \mu l^3 / 6 \ln(2/\epsilon)$ [52,57]. Note that Eq. (15) for $\mathbf{S}^b(\mathbf{p})$ strictly represents the stress exerted by a particle undergoing random rotations as a result of Brownian motion: it is therefore unclear that it is also applicable to model the stress resulting from tumbling of a swimming bacterium, for instance. In cases where rotary diffusion is used to model tumbling in Eq. (1), $\mathbf{S}^b(\mathbf{p})$ should therefore be set to zero. We carry it along in this study, noting that setting it to zero is simply equivalent to modifying the numerical value of the swimming stresslet strength σ_0 introduced below, and therefore does not qualitatively change the results of this analysis.

Finally, the force dipole resulting from swimming can be expressed in the form [24,25,50]

$$\mathbf{S}^s(\mathbf{p}) = \sigma_0 \left[\mathbf{pp} - \frac{\mathbf{I}}{3} \right], \tag{16}$$

where the dipole or stresslet strength σ_0 is a constant depending on the mechanism for swimming and can be interpreted as a measure of activity. Note that σ_0 can be either positive or negative depending on the type of swimmer: for tail-actuated particles or *pushers* such as most swimming bacteria (e.g., *Escherichia Coli* and *Bacillus Subtilis*), it can be shown that $\sigma_0 < 0$; conversely, $\sigma_0 > 0$ for head-actuated swimmers or *pullers* such as the alga *Chlamydomonas Reinhardtii*. In addition, it can be shown by dimensional analysis or using more detailed models for microswimmers that σ_0 is

related to the swimming speed U_0 and size l of the particles by a relation of the type $\sigma_0/\mu U_0 l^2=\alpha$, where α is a dimensionless constant of the same sign as σ_0, e.g., see [25,31].

Substituting Eqs. (14)–(16) into Eq. (12) yields an expression for the particle extra stress,

$$\boldsymbol{\Sigma}^p = \frac{\pi\mu(nl^3)}{6\ln(2/\epsilon)}\left[\langle \mathbf{pppp}\rangle - \frac{\mathbf{I}}{3}\langle \mathbf{pp}\rangle\right]:\mathbf{E} + (3nkT + n\sigma_0)\left[\langle \mathbf{pp}\rangle - \frac{\mathbf{I}}{3}\right]. \tag{17}$$

This can be further simplified by making use of the following identity, which can be derived from the steady-state Fokker-Planck equation [53],

$$\langle \mathbf{pppp}\rangle:\mathbf{E} = \langle \mathbf{pp}\rangle\cdot\mathbf{E} - \frac{d}{\beta}(3\langle \mathbf{pp}\rangle - \mathbf{I}), \tag{18}$$

yielding

$$\boldsymbol{\Sigma}^p = \frac{\pi\mu(nl^3)}{6\ln(2/\epsilon)}\left\{\left[\langle \mathbf{pp}\rangle\cdot\mathbf{E} - \frac{\mathbf{I}}{3}\langle \mathbf{pp}\rangle:\mathbf{E}\right] + 3d\left(2 + 2\tilde{\sigma}_0 - \frac{1}{\beta}\right)\left[\langle \mathbf{pp}\rangle - \frac{\mathbf{I}}{3}\right]\right\}. \tag{19}$$

To obtain Eq. (19), we also made use of the following relation between A and d, valid for a slender particle: $2Ad=kT$. We also defined a dimensionless activity $\tilde{\sigma}_0$ as

$$\tilde{\sigma}_0 = \frac{\sigma_0}{3kT}. \tag{20}$$

In Eq. (19), nl^3 plays the role of an effective volume fraction, which may be significantly higher than the actual volume fraction in the case of high-aspect-ratio particles, but is the appropriate measure of concentration for determining the importance of hydrodynamic interactions in such suspensions [41,61]; the dilute regime of interest here, in which hydrodynamic interactions can be neglected, occurs when $nl^3 \ll 1$. Note that because nl^3 is typically large compared to the actual volume fraction, this restriction is quite strong and the theory presented here is really only expected to be accurate at very low volume fractions, at which the effects of the particles on the rheology may be weak. However, studies on passive rod suspensions suggest that theoretical results obtained in the dilute limit of $nl^3 \ll 1$ are often valid up to $nl^3 \sim O(1)$ and beyond, at least qualitatively, e.g., [62].

From Eq. (19), we see that the particle extra stress is entirely determined from the second moment $\langle \mathbf{pp}\rangle$ of the orientation distribution $\Psi(\mathbf{p})$. In the following sections, we analyze the cases of uniaxial extensional and compressional flows and of planar extensional flow, and we show that $\langle \mathbf{pp}\rangle$ and $\boldsymbol{\Sigma}^p$ can both be obtained analytically.

III. AXISYMMETRIC FLOWS

We first consider the case of uniaxial straining flows, for which the rate-of-strain tensor has the following form:

$$\mathbf{E} = \dot{\epsilon}\begin{bmatrix} -\frac{1}{2} & 0 & 0 \\ 0 & -\frac{1}{2} & 0 \\ 0 & 0 & 1 \end{bmatrix}, \tag{21}$$

where $\dot{\epsilon}$ is the strain rate. The sign of $\dot{\epsilon}$ determines the flow type: $\dot{\epsilon}>0$ corresponds to an extensional flow, whereas $\dot{\epsilon}<0$ corresponds to a compressional flow. We also define an effective Péclet number, or dimensionless flow strength, as $\mathrm{Pe}=\dot{\epsilon}/d$. Pe compares the effects of the external flow and of rotary diffusion on the orientational dynamics of a particle. In cases where rotary diffusion is used as a model for hydrodynamic fluctuations or for tumbling, it may also depend indirectly on the suspension concentration or on the correlation time for tumbling, respectively, through the value of the effective rotary diffusivity d.

Using spherical coordinate angles (θ,ϕ) with polar axis in the z direction (with $\theta\in[0,\pi]$ and $\phi\in[0,2\pi)$), the particle director can be parametrized as

$$\mathbf{p} = [\sin\theta\cos\phi, \sin\theta\sin\phi, \cos\phi]. \tag{22}$$

In this case, the orientation distribution is axisymmetric, $\Psi(\mathbf{p})=\Psi(\theta)$, and solution (9) of the steady-state Fokker-Planck equation (4) simplifies to

$$\Psi(\theta) = \frac{1}{K}\exp\left(\frac{3}{4}\lambda\cos^2\theta\right), \tag{23}$$

where $\lambda=\beta\dot{\epsilon}/d=\beta\,\mathrm{Pe}$, and K is given by

$$K = 2\pi\int_0^\pi \exp\left(\frac{3}{4}\lambda\cos^2\theta\right)\sin\theta d\theta. \tag{24}$$

An analytical expression for K was obtained by Brenner and Condiff [53] as

$$K = \begin{cases} 4\pi\xi^{-1}\exp(\xi^2)D(\xi) & \text{for } \lambda>0 \\ 2\pi^{3/2}\xi^{-1}\,\mathrm{erf}\,\xi & \text{for } \lambda<0, \end{cases} \tag{25}$$

where $\xi=|3\lambda/4|^{1/2}$, $D(\xi)$ is Dawson's integral [63], and erf ξ is the error function. Figure 1 shows typical orientation distributions for both extensional and compressional flows, for various flow strengths λ. In extensional flows ($\lambda>0$), the particles are found to align along the extensional axis as expected, with a stronger degree of alignment at high flow rates (high λ). In compressional flows, however, alignment does not occur; instead, the particles orient perpendicular to the compressional axis, with no preferred azimuthal direction.

Knowing the orientation distribution $\Psi(\theta)$, we can determine its second moment $\langle \mathbf{pp}\rangle$ as

$$\langle \mathbf{pp}\rangle = \begin{bmatrix} \frac{1}{2}(1-M) & 0 & 0 \\ 0 & \frac{1}{2}(1-M) & 0 \\ 0 & 0 & M \end{bmatrix}, \tag{26}$$

where

$$M = 2\pi\int_0^\pi \Psi(\theta)\cos^2\theta\sin\theta d\theta. \tag{27}$$

In particular, M can be evaluated as [53]

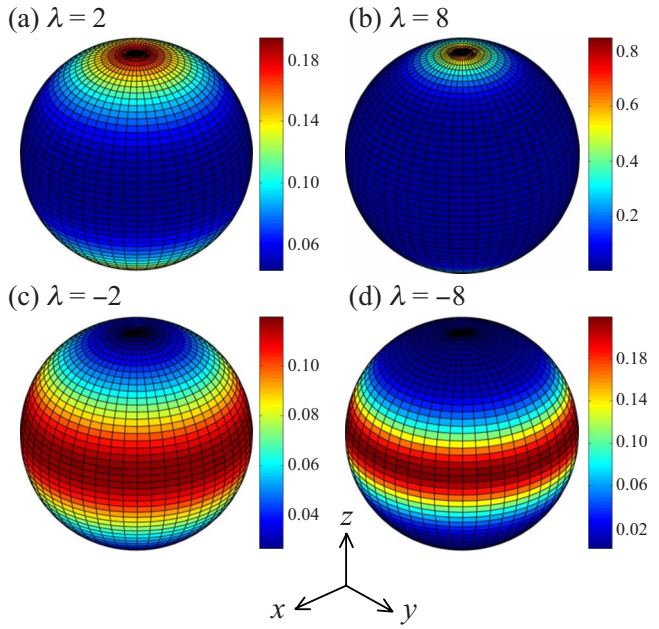

FIG. 1. (Color online) Steady-state orientation distributions $\Psi(\mathbf{p})$ in uniaxial [(a) and (b)] extensional and [(c) and (d)] compressional flows, for various flow strengths $\lambda=\beta\dot{\epsilon}/d=\beta\,\mathrm{Pe}$, obtained from Eq. (23).

$$M=\begin{cases}\dfrac{1}{2\xi D(\xi)}-\dfrac{1}{2\xi^2} & \text{for } \lambda>0\\[2ex] \dfrac{1}{2\xi^2}-\dfrac{\exp(-\xi^2)}{\pi^{1/2}\xi\,\mathrm{erf}\,\xi} & \text{for } \lambda<0.\end{cases} \tag{28}$$

The second moment $\langle\mathbf{pp}\rangle$ can then be substituted into Eq. (19) to determine the particle extra stress $\mathbf{\Sigma}^p$. After manipulation, we find that $\mathbf{\Sigma}^p$ is of the form

$$\mathbf{\Sigma}^p=2(nl^3)\mu\eta_p\mathbf{E}, \tag{29}$$

where nl^3 is the effective volume fraction. The dimensionless coefficient η_p is the intrinsic viscosity of the suspension, which is straightforward to obtain as

$$\eta_p=\frac{\pi}{12\,\ln(2/\epsilon)}\left[\frac{1}{2}\left(M+\frac{1}{3}\right)+\frac{3}{\mathrm{Pe}}\left(2+2\tilde{\sigma}_0-\frac{1}{\beta}\right)\left(M-\frac{1}{3}\right)\right], \tag{30}$$

where M is given by Eq. (28). In particular, Eq. (29) shows that the suspension behaves like a Newtonian fluid with a strain-rate-dependent viscosity; normal stresses do not occur. This conclusion is the same as that found by Brenner [54] for passive suspensions, and only holds for axisymmetric flows. Asymptotic expressions for η_p can also be obtained in the weak and strong flow limits by expanding M in the appropriate limits, and are given by

$$\eta_p=\frac{\pi}{12\,\ln(2/\epsilon)}\begin{cases}\dfrac{2}{15}+\dfrac{\beta}{5}(2+2\tilde{\sigma}_0)+O(\mathrm{Pe}) & \text{as } \mathrm{Pe}\to 0\\[2ex] \dfrac{2}{3}+2\left(2+2\tilde{\sigma}_0-\dfrac{4}{3\beta}\right)\mathrm{Pe}^{-1}+O(\mathrm{Pe}^{-2}) & \text{as } \mathrm{Pe}\to+\infty\\[2ex] \dfrac{1}{6}-\left(2+2\tilde{\sigma}_0-\dfrac{2}{3\beta}\right)\mathrm{Pe}^{-1}+O(\mathrm{Pe}^{-2}) & \text{as } \mathrm{Pe}\to-\infty.\end{cases} \tag{31}$$

The intrinsic viscosity (30) is plotted versus Péclet number in Fig. 2 for suspensions of passive particles, pushers, and pullers. In the passive case ($\tilde{\sigma}_0=0$), the viscosity exhibits strain-rate thinning in compressional flows, and strain-rate thickening in extensional flows, in agreement with previous well-established results [54]. The effect of activity is strongest in weak flows (low Péclet numbers), where it results in an enhancement of η_p in suspensions of pullers ($\tilde{\sigma}_0>0$) but in a decrease in η_p in suspensions of pushers ($\tilde{\sigma}_0<0$). In suspensions of pullers, this results in strain-rate thinning in strong extensional flows. The effect of activity, however, is most drastic in suspensions of pushers, where the intrinsic viscosity is seen to become negative in weak flows when $\tilde{\sigma}_0$ is strongly negative; the viscosity therefore remains strain-rate thickening in extensional flows, but becomes strain-rate thickening in compressional flows as well. A negative particle viscosity had already been predicted in other studies [48–50], including in shear flow [50], and has also been reported in experiments [44]: it appears to be a general feature of strongly active suspensions in weak flows.

This feature is further analyzed in Fig. 3, showing the range of activities $\tilde{\sigma}_0$ and Péclet numbers Pe for which $\eta_p<0$. Confirming the results of Fig. 2, we find that negative intrinsic viscosities occur in weak flows (small values of Pe) of strongly active suspensions of pushers (large negative values of $\tilde{\sigma}_0$). Interestingly, we also find that negative viscosities are more likely to occur in compressional flows than in extensional flows.

IV. PLANAR FLOWS

We next consider planar extensional flows, for which the rate-of-strain tensor is of the form

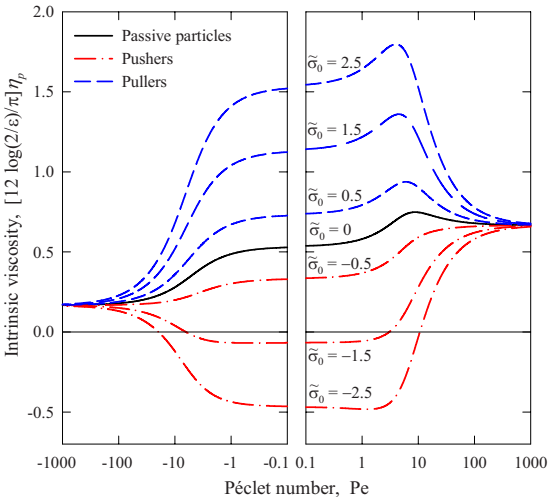

FIG. 2. (Color online) Intrinsic viscosity η_p normalized by $\pi/12\ln(2/\epsilon)$ versus Péclet number $\mathrm{Pe}=\dot{\varepsilon}/d$ in suspensions of slender particles ($\beta=1$) in uniaxial flow, obtained from Eq. (30). The various curves correspond to suspensions of passive particles ($\tilde{\sigma}_0=0$), as well as active suspensions of pushers ($\tilde{\sigma}_0<0$) and pullers ($\tilde{\sigma}_0>0$) at various levels of activity. Negative values of Pe correspond to compressional flow, whereas positive values correspond to extensional flow.

$$\mathbf{E}=\dot{\varepsilon}\begin{bmatrix}\frac{1}{2} & 0 & 0\\ 0 & -\frac{1}{2} & 0\\ 0 & 0 & 0\end{bmatrix}. \tag{32}$$

Note that changing the sign of $\dot{\varepsilon}$ simply reverses the roles of the x and y axes, so that we can assume that $\dot{\varepsilon}>0$ without loss of generality. In this case, the orientation distribution is no longer axisymmetric. Using the same spherical coordinate system as in Sec. III, the steady-state orientation distribution becomes

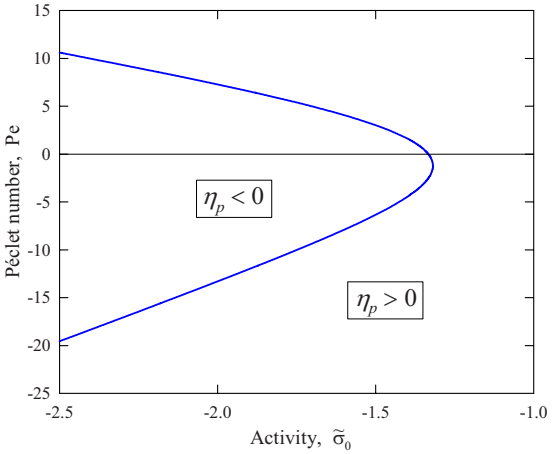

FIG. 3. (Color online) Critical flow strength (measured by the Péclet number Pe) below which negative intrinsic viscosities η_p occur, as a function of activity $\tilde{\sigma}_0$, in uniaxial extensional ($\mathrm{Pe}>0$) and compressional ($\mathrm{Pe}<0$) flows.

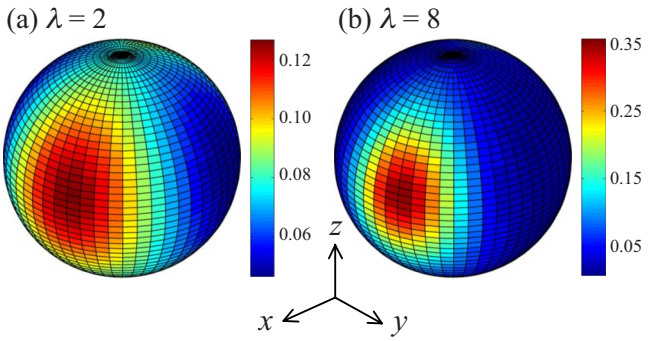

FIG. 4. (Color online) Steady-state orientation distributions $\Psi(\mathbf{p})$ in planar extensional flow, for two different flow strengths $\lambda=\beta\dot{\varepsilon}/d=\beta\,\mathrm{Pe}$, obtained from Eq. (33).

$$\Psi(\theta,\phi)=\frac{1}{K}\exp\left(\frac{1}{4}\lambda\,\sin^2\theta\cos 2\phi\right), \tag{33}$$

with λ still defined as $\lambda=\beta\dot{\varepsilon}/d=\beta\,\mathrm{Pe}$. The normalization constant K in this case is given by

$$K=\int_0^{2\pi}\int_0^{\pi}\exp\left(\frac{1}{4}\lambda\,\sin^2\theta\cos 2\phi\right)\sin\theta\,d\theta\,d\phi, \tag{34}$$

and was obtained by Brenner and Condiff [53] as

$$K=2^{1/2}\pi^2 I_{1/4}(\xi)I_{-1/4}(\xi), \tag{35}$$

where $\xi=\lambda/8$, and I_ν denotes the modified Bessel function of the first kind of order ν. Steady-state orientation distributions in this case are shown in Fig. 4, where alignment along the extensional axis (x axis) occurs as expected and becomes stronger as the Péclet number increases.

The determination of the stress in this case is slightly more cumbersome. First we express the second moment $\langle\mathbf{pp}\rangle$ of the orientation distribution as

$$\langle\mathbf{pp}\rangle=\begin{bmatrix}\langle\sin^2\theta\cos^2\phi\rangle & 0 & 0\\ 0 & \langle\sin^2\theta\sin^2\phi\rangle & 0\\ 0 & 0 & \langle\cos^2\theta\rangle\end{bmatrix}, \tag{36}$$

or, equivalently,

$$\langle\mathbf{pp}\rangle=\begin{bmatrix}\frac{1}{2}(g+h) & 0 & 0\\ 0 & \frac{1}{2}(h-g) & 0\\ 0 & 0 & 1-h\end{bmatrix}, \tag{37}$$

where $g=\langle\sin^2\theta\cos 2\phi\rangle$ and $h=\langle\sin^2\theta\rangle$. Both g and h were obtained in terms of $\xi=\lambda/8$ by Brenner and Condiff as follows [53]:

$$g=\frac{I_{1/4}(\xi)I'_{-1/4}(\xi)+I_{-1/4}(\xi)I'_{1/4}(\xi)}{2I_{1/4}(\xi)I_{-1/4}(\xi)}, \tag{38}$$

$$h=\frac{I_{1/4}(\xi)I_{-1/4}(\xi)+I_{3/4}(\xi)I_{-3/4}(\xi)}{2I_{1/4}(\xi)I_{-1/4}(\xi)}. \tag{39}$$

Substituting Eq. (37) into Eq. (19) yields the particle extra stress. In this case, $\boldsymbol{\Sigma}^p$ is not proportional to the rate-of-strain

tensor, i.e., normal stresses will arise. We define the dimensionless intrinsic viscosity η_p and normal stress function σ_p as

$$\eta_p = \frac{\Sigma^p_{xx} - \Sigma^p_{yy}}{2\mu(nl^3)\dot{\varepsilon}}, \quad \sigma_p = \frac{\Sigma^p_{xx} + \Sigma^p_{yy} - 2\Sigma^p_{zz}}{2\mu(nl^3)\dot{\varepsilon}}. \tag{40}$$

These are easily determined from $\mathbf{\Sigma}^p$ as

$$\eta_p = \frac{\pi}{12\ln(2/\epsilon)}\left[\frac{h}{2} + \frac{3}{\mathrm{Pe}}\left(2 + 2\tilde{\sigma}_0 - \frac{1}{\beta}\right)g\right], \tag{41}$$

$$\sigma_p = \frac{\pi}{12\ln(2/\epsilon)}\left[\frac{g}{2} + \frac{3}{\mathrm{Pe}}\left(2 + 2\tilde{\sigma}_0 - \frac{1}{\beta}\right)(3h-2)\right], \tag{42}$$

and asymptotic expressions in the weak and strong flow limits can also be obtained as

$$\eta_p = \frac{\pi}{12\ln(2/\epsilon)} \times \begin{cases} \dfrac{2}{15} + \dfrac{\beta}{5}(2 + 2\tilde{\sigma}_0) + O(\mathrm{Pe}) & \text{as } \mathrm{Pe} \to 0 \\ \dfrac{1}{2} + 3\left(2 + 2\tilde{\sigma}_0 - \dfrac{4}{3\beta}\right)\mathrm{Pe}^{-1} + O(\mathrm{Pe}^{-2}) & \text{as } \mathrm{Pe} \to +\infty, \end{cases} \tag{43}$$

$$\sigma_p = \frac{\pi}{12\ln(2/\epsilon)} \times \begin{cases} \left[\dfrac{2\beta}{105} + \dfrac{\beta^2}{70}(2 + 2\tilde{\sigma}_0)\right]\mathrm{Pe} + O(\mathrm{Pe}^2) & \text{as } \mathrm{Pe} \to 0 \\ \dfrac{1}{2} + 3\left(2 + 2\tilde{\sigma}_0 - \dfrac{5}{3\beta}\right)\mathrm{Pe}^{-1} + O(\mathrm{Pe}^{-2}) & \text{as } \mathrm{Pe} \to +\infty. \end{cases} \tag{44}$$

Figure 5 shows both η_p and σ_p as functions of the Péclet number for passive particles, pushers, and pullers. For passive particles ($\tilde{\sigma}_0$=0), the intrinsic viscosity exhibits weak strain-rate thickening at low Pe followed by strain-rate thinning at high Pe but is nearly constant over the range of Péclet numbers considered here; normal stresses, which tend toward zero in the weak flow limit, increase to a finite positive value in strong flows [54]. In the case of pullers ($\tilde{\sigma}_0 > 0$), activity enhances the zero-strain-rate viscosity, resulting in strain-rate thinning; it also results in an enhancement of the normal stress function at intermediate flow strengths. The effects in the case of suspensions of pushers ($\tilde{\sigma}_0 < 0$) are reversed. The zero-strain-rate viscosity decreases as a result of activity, causing η_p to become negative at low values of Pe if $\tilde{\sigma}_0$ is sufficiently negative, in qualitative agreement with our observations in Sec. III for axisymmetric flows. Activity in suspensions of pushers also causes a decrease in the normal stress function at moderate flow strengths, causing it to change sign and become negative at low and intermediate values of Pe in the case of strongly active suspensions.

The negative intrinsic viscosity occurring in suspensions of pushers is further characterized in Fig. 6(a), showing the critical flow strength below which $\eta_p < 0$ as a function of activity $\tilde{\sigma}_0$. As in the case of uniaxial extensional and compressional flows (Fig. 3), we find that a negative effective viscosity will occur in weak flows (low values of Pe) of strongly active pusher suspensions (high values of $|\tilde{\sigma}_0|$). Similarly, Fig. 6(b) shows the critical flow strength at which σ_p changes sign in suspensions of pushers: negative normal stress functions also primarily occur in weak flows.

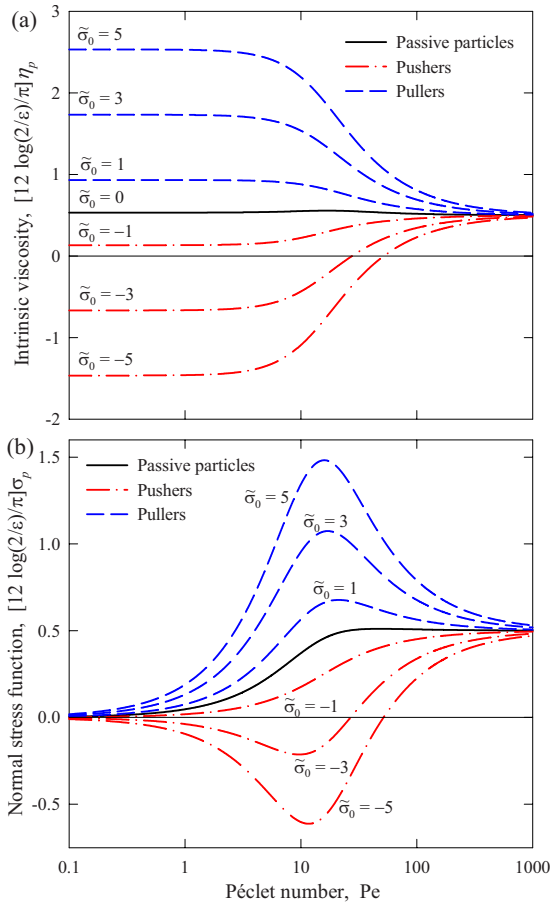

FIG. 5. (Color online) Intrinsic viscosity η_p and normal stress function σ_p normalized by $\pi/12\ln(2/\epsilon)$ versus Péclet number $\mathrm{Pe}=\dot{\varepsilon}/d$ in suspensions of slender particles (β=1) in planar extensional flow, obtained from Eq. (40). The various curves correspond to suspensions of passive particles ($\tilde{\sigma}_0$=0), as well as active suspensions of pushers ($\tilde{\sigma}_0 < 0$) and pullers ($\tilde{\sigma}_0 > 0$) at various levels of activity.

V. ENERGY DISSIPATION AND ACTIVE POWER INPUT

As we demonstrated in Figs. 2 and 5, and as previously observed in other theoretical [46,48–50] and experimental [44] studies, active suspensions of pusher particles can exhibit negative particle viscosities η_p in weak flows at strong levels of activity. While η_p only represents the first correction to the Newtonian viscosity as a result of activity, a negative value of η_p still means a decrease in the overall suspension viscosity, which seems to suggest an unphysical reduction in viscous dissipation due to the particle phase. In reality, this apparent reduction in viscous dissipation is easily explained by realizing that the contribution to the particle

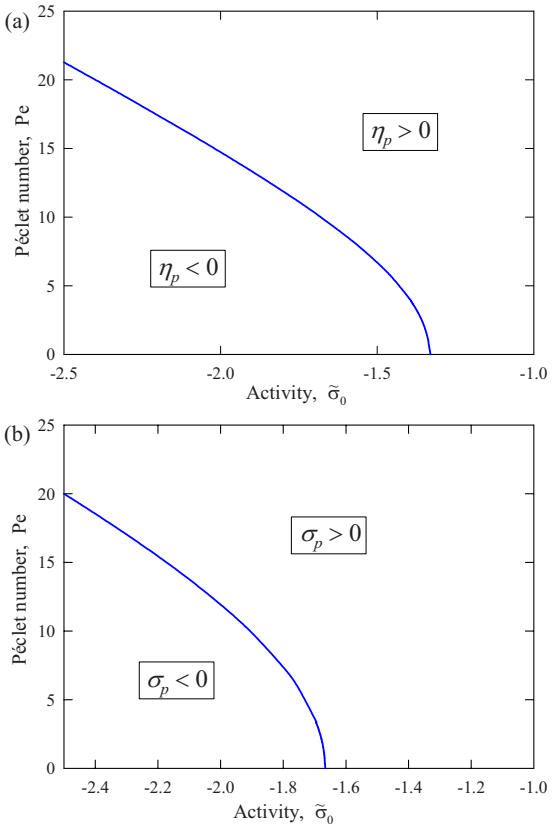

FIG. 6. (Color online) (a) Critical flow strength (measured by the Péclet number Pe) below which negative intrinsic viscosities η_p occur, as a function of activity $\tilde{\sigma}_0$, in planar extensional flow of a pusher suspension. (b) Critical flow strength below which a negative normal stress function σ_p occurs, as a function of activity $\tilde{\sigma}_0$, in planar extensional flow of a pusher suspension.

stress due to swimming is not dissipative in nature, but arises due to the activity of the particles, which are constantly injecting mechanical energy into the fluid. To analyze this effect in more detail, we perform an energy balance in the spirit of Landau and Lifschitz [64]. We consider the flow of an active suspension in a finite domain D bounded by fixed no-slip boundaries, governed by the unsteady Cauchy equation in which we use the total stress of Eq. (11),

$$\rho \frac{D\mathbf{u}}{Dt} = \boldsymbol{\nabla} \cdot (-q\mathbf{I} + 2\mu\mathbf{E} + \boldsymbol{\Sigma}^p). \tag{45}$$

In Eq. (45), $\mathbf{u}$ is the fluid velocity with rate-of-strain tensor $\mathbf{E}=(\boldsymbol{\nabla}\mathbf{u}+\boldsymbol{\nabla}\mathbf{u}^T)/2$, and D/Dt denotes the material derivative. Taking the dot product of Eq. (45) with $\mathbf{u}$ and integrating over the domain D yields after integration by parts and using the symmetry of $\mathbf{E}$ [64]

$$\frac{dE_k}{dt} = -2\mu \int_D \mathbf{E}:\mathbf{E}dV - \int_D \boldsymbol{\Sigma}^p:\mathbf{E}dV, \tag{46}$$

where E_k denotes the kinetic energy of the flow,

$$E_k = \frac{1}{2}\rho \int_D |\mathbf{u}|^2 dV. \tag{47}$$

Note that the energy balance of Eq. (46) only concerns the mechanical energy associated with the macroscale flow driven by the swimming particles on length scales much larger than l (for the expression for the stress tensor to be valid): it does not represent a full energy balance for all the microscale processes involved with particle propulsion, which would include additional damping contributions and should also account for the precise source of energy of the particles (e.g., bacterial metabolism). With this in mind, the first term on the right-hand side of Eq. (46) is always negative and corresponds to the rate of viscous dissipation Φ in the Newtonian suspending fluid,

$$\Phi = 2\mu \int_D \mathbf{E}:\mathbf{E}dV \geq 0. \tag{48}$$

The second term includes contributions from the various particle stresses [Eqs. (14)–(16)]. It can be decomposed as

$$\int_D \boldsymbol{\Sigma}^p:\mathbf{E}dV = \underbrace{\int_D \boldsymbol{\Sigma}^f:\mathbf{E}dV}_{\Phi_f} + \underbrace{\int_D \boldsymbol{\Sigma}^b:\mathbf{E}dV}_{\Phi_b} + \underbrace{\int_D \boldsymbol{\Sigma}^s:\mathbf{E}dV}_{\Phi_s}. \tag{49}$$

The first two terms Φ_f and Φ_b, arising from $\boldsymbol{\Sigma}^f$ and $\boldsymbol{\Sigma}^b$, are both dissipative and must be positive: they correspond to the rates of energy dissipation induced by the inextensibility of the particles and by Brownian rotations, both of which result in extra friction and viscous dissipation near the particle surfaces. The third term Φ_s, however, has a different interpretation: $\mathcal{P}=-\Phi_s$ defines the active power input induced by the permanent dipoles exerted by the particles as they swim through the fluid (see [25]). It is not a dissipative term, but rather accounts for the rate of mechanical energy generated by the swimming particles: the sign of Φ_s may therefore be negative depending on the mechanism for swimming.

If we assume that $\mathbf{E}$ is given by Eq. (21), i.e., that the fluid flow is locally a uniaxial extensional or compressional flow, the various integrands on the right-hand side of Eq. (49) can be calculated as

$$\phi_f = \boldsymbol{\Sigma}^f:\mathbf{E} = \phi_0\left[\frac{1}{2}\left(M+\frac{1}{3}\right) - \frac{3}{\beta\,\mathrm{Pe}}\left(M-\frac{1}{3}\right)\right], \tag{50}$$

$$\phi_b = \boldsymbol{\Sigma}^b:\mathbf{E} = \phi_0\left[\frac{6}{\mathrm{Pe}}\left(M-\frac{1}{3}\right)\right], \tag{51}$$

$$\phi_s = \boldsymbol{\Sigma}^s:\mathbf{E} = \phi_0\left[\frac{6\tilde{\sigma}_0}{\mathrm{Pe}}\left(M-\frac{1}{3}\right)\right], \tag{52}$$

where $\phi_0=\pi\mu(nl^3)\dot{\epsilon}^2/4\ln(2/\epsilon)$. Note also that the intrinsic viscosity of Eq. (30) is related to ϕ_f, ϕ_b, and ϕ_s by

$$\eta_p = \frac{2}{3\mu(nl^3)\dot{\epsilon}^2}(\phi_f + \phi_b + \phi_s). \tag{53}$$

Figure 7 shows ϕ_f, ϕ_b, ϕ_s, and their sum as functions of Péclet number in a uniaxial extensional flow for a suspension

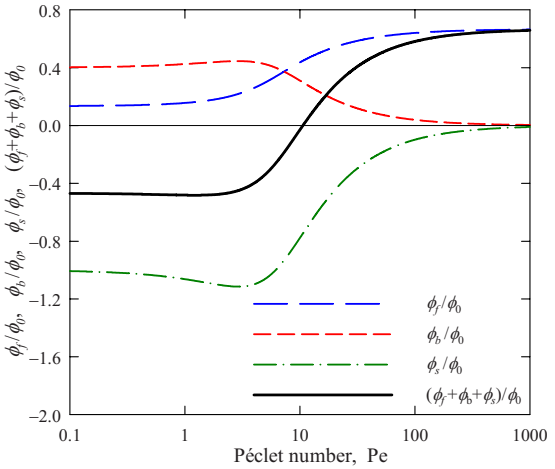

FIG. 7. (Color online) Integrands ϕ_f, ϕ_b, ϕ_s appearing in Eq. (49), and their sum, as functions of Péclet number in uniaxial extensional flow of an active suspension of slender pushers ($\beta=1$, $\tilde{\sigma}_0=-2.5$). They were calculated based on Eqs. (50)–(52) and are scaled by $\phi_0=\pi\mu(nl^3)\dot{\epsilon}^2/4\ \ln(2/\epsilon)$.

of pushers with $\tilde{\sigma}_0=-2.5$. In particular, ϕ_f and ϕ_b are found to be positive for all values of Pe, as expected since they represent the extra viscous dissipation due to particle inextensibility and Brownian rotations. We find however that $\phi_s<0$, corresponding to a positive active power input. The sum of ϕ_f, ϕ_b, and ϕ_s, which is related to the intrinsic viscosity via Eq. (53), can therefore be either positive or negative depending on the relative magnitude of the various terms: a negative intrinsic viscosity η_p is obtained at low values of Pe when the active power input dominates viscous dissipation, whereas a positive η_p occurs in stronger flows when viscous dissipation is the dominant contribution to the sum. In particular, this analysis identifies the active power input generated by the particles as the origin of the negative intrinsic viscosities predicted at low Pe, and it clearly shows that negative values of η_p do not violate the requirement of a positive rate of viscous dissipation as η_p includes a contribution which is not of dissipative origin. In fact, the active power input identified in Eq. (46) via Eq. (49) can sometimes result in an increase in kinetic energy by driving disturbance flows even in the absence of any external forcing, as seen in previous studies on hydrodynamic interactions in active suspensions, e.g., [24,25].

VI. CONCLUDING REMARKS

We have presented a simple kinetic model for the effective rheology of an active suspension in irrotational flows, which extends classic theories for passive particle suspensions [54]. The model is similar to that previously used in [50] for steady shear flows and is based on the assumption of diluteness ($nl^3\ll 1$), by which particle-particle interactions can be entirely neglected. Under this assumption, the configuration of the suspension is modeled via an orientation distribution, which satisfies a Fokker-Planck equation and can be solved for analytically in the case of an imposed irrotational flow. The particle extra stress is then obtained using this orientation distribution as a configurational average of the force dipoles on the particles, which include a permanent dipole resulting from activity. Analytical expressions were obtained for the intrinsic viscosity in uniaxial extensional and compressional flows as well as in planar extensional flow: in all cases, we found that activity results in an increase in the intrinsic viscosity in suspensions of pullers, but in a decrease in suspensions of pushers, which can result in a negative intrinsic viscosity in weak flows and strongly active suspensions. These predictions are consistent with previous theoretical models [46,48–50] and are also in agreement with experimental studies, which have demonstrated a viscosity enhancement in suspensions of pullers [45] but a reduction in suspensions of pushers [44]. Using a simple energy balance, we also identified the active power input generated by swimming particles (a nondissipative process) as the origin for the decrease in viscosity predicted in pusher suspensions.

Of great interest in active suspensions is the role of hydrodynamic interactions induced by the permanent swimming dipoles: these indeed result in very complex dynamics, pattern formation, unsteady chaotic flows, mixing and diffusion, e.g., see [24,25]. These phenomena were completely neglected in the present theory, which focused on the leading effect of activity in dilute suspensions. Beyond the dilute regime, they will have to be taken into account and are likely to quantitatively modify the results presented herein. In particular, particle orientation distributions are likely to become spatially dependent and unsteady, with similar conclusions for the particle extra stress. Recent kinetic simulations in shear flow suggest that these phenomena will become important in weak flows, but may disappear in stronger flows, which are found to be stabilizing [65]: the subtle effects of concentration on the effective rheology can therefore hardly be anticipated and will require additional work.

ACKNOWLEDGMENTS

The author is grateful to M. J. Shelley and A. S. Khair for useful conversations. This work was supported by NSF Grant No. DMS-0920931 under the American Recovery and Reinvestment Act.

[1] E. M. Purcell, Am. J. Phys. **45**, 3 (1977).
[2] C. Brennen and H. Winet, Annu. Rev. Fluid Mech. **9**, 339 (1977).
[3] W. F. Paxton, K. C. Kistler, C. C. Olmeda, A. Sen, S. K. St. Angelo, Y. Cao, T. E. Mallouk, P. E. Lammert, and V. H. Crespi, J. Am. Chem. Soc. **126**, 13424 (2004).
[4] R. Golestanian, T. B. Liverpool, and A. Ajdari, Phys. Rev. Lett. **94**, 220801 (2005).

[5] T. Mallouk and A. Sen, Sci. Am. **300**, 72 (2009).
[6] R. Dreyfus, J. Baudry, M. L. Roper, H. A. Stone, M. Fermigier, and J. Bibette, Nature (London) **437**, 862 (2005).
[7] E. E. Keaveny and M. R. Maxey, J. Fluid Mech. **598**, 293 (2008).
[8] W. M. Durham, J. O. Kessler, and R. Stocker, Science **323**, 1067 (2009).
[9] J. R. Seymour, Marcos, and R. Stocker, Am. Nat. **173**, E15 (2009).
[10] M. Parsek and P. Singh, Annu. Rev. Microbiol. **57**, 677 (2003).
[11] M. J. Kim and K. S. Breuer, Phys. Fluids **16**, L78 (2004).
[12] N. Darnton, L. Turner, K. Breuer, and H. C. Berg, Biophys. J. **86**, 1863 (2004).
[13] E. Lauga and T. R. Powers, Rep. Prog. Phys. **72**, 096601 (2009).
[14] J. J. L. Higdon, J. Fluid Mech. **90**, 685 (1979).
[15] T. S. Yu, E. Lauga, and A. E. Hosoi, Phys. Fluids **18**, 091701 (2006).
[16] A. Ajdari and H. A. Stone, Phys. Fluids **11**, 1275 (1999).
[17] E. Gouin, M. D. Welch, and P. Cossart, Curr. Opin. Microbiol. **8**, 35 (2005).
[18] A. M. Leshansky, Phys. Rev. E **74**, 012901 (2006).
[19] D. Bartolo and E. Lauga, Phys. Rev. E **81**, 026312 (2010).
[20] R. A. Simha and S. Ramaswamy, Phys. Rev. Lett. **89**, 058101 (2002).
[21] J. P. Hernandez-Ortiz, C. G. Stoltz, and M. D. Graham, Phys. Rev. Lett. **95**, 204501 (2005).
[22] P. T. Underhill, J. P. Hernandez-Ortiz, and M. D. Graham, Phys. Rev. Lett. **100**, 248101 (2008).
[23] J. P. Hernandez-Ortiz, P. T. Underhill, and M. D. Graham, J. Phys.: Condens. Matter **21**, 204107 (2009).
[24] D. Saintillan and M. J. Shelley, Phys. Rev. Lett. **100**, 178103 (2008).
[25] D. Saintillan and M. J. Shelley, Phys. Fluids **20**, 123304 (2008).
[26] C. Hohenegger and M. J. Shelley, Phys. Rev. E **81**, 046311 (2010).
[27] V. Mehandia and P. R. Nott, J. Fluid Mech. **595**, 239 (2008).
[28] G. Subramanian and D. L. Koch, J. Fluid Mech. **632**, 359 (2009).
[29] A. Baskaran and M. C. Marchetti, Proc. Natl. Acad. Sci. U.S.A. **106**, 15567 (2009).
[30] I. S. Aranson, A. Sokolov, J. O. Kessler, and R. E. Goldstein, Phys. Rev. E **75**, 040901(R) (2007).
[31] D. Saintillan and M. J. Shelley, Phys. Rev. Lett. **99**, 058102 (2007).
[32] T. Ishikawa, M. P. Simmonds, and T. J. Pedley, J. Fluid Mech. **568**, 119 (2006).
[33] T. Ishikawa and T. J. Pedley, Phys. Rev. Lett. **100**, 088103 (2008).
[34] X.-L. Wu and A. Libchaber, Phys. Rev. Lett. **84**, 3017 (2000).
[35] N. H. Mendelson, A. Bourque, K. Wilkening, K. R. Anderson, and J. C. Watkins, J. Bacteriol. **181**, 600 (1999).
[36] G. V. Soni, B. M. Jaffar Ali, Y. Hatwalne, and G. V. Shivashankar, Biophys. J. **84**, 2634 (2003).
[37] C. Dombrowski, L. Cisneros, S. Chatkaew, R. E. Goldstein, and J. O. Kessler, Phys. Rev. Lett. **93**, 098103 (2004).
[38] I. Tuval, L. Cisneros, C. Dombrowski, C. W. Wolgemuth, J. O. Kessler, and R. E. Goldstein, Proc. Natl. Acad. Sci. U.S.A. **102**, 2277 (2005).
[39] A. Sokolov, I. S. Aranson, J. O. Kessler, and R. E. Goldstein, Phys. Rev. Lett. **98**, 158102 (2007).
[40] J. H. Irving and J. G. Kirkwood, J. Chem. Phys. **18**, 817 (1950).
[41] M. Doi and S. F. Edwards, *The Theory of Polymer Dynamics* (Oxford University Press, New York, 1986).
[42] G. K. Batchelor, J. Fluid Mech. **46**, 813 (1971).
[43] G. K. Batchelor, Annu. Rev. Fluid Mech. **6**, 227 (1974).
[44] A. Sokolov and I. S. Aranson, Phys. Rev. Lett. **103**, 148101 (2009).
[45] S. Rafaï, L. Jibuti, and P. Peyla, Phys. Rev. Lett. **104**, 098102 (2010).
[46] Y. Hatwalne, S. Ramaswamy, M. Rao, and R. A. Simha, Phys. Rev. Lett. **92**, 118101 (2004).
[47] T. Ishikawa and T. J. Pedley, J. Fluid Mech. **588**, 399 (2007).
[48] B. M. Haines, I. S. Aranson, L. Berlyand, and D. A. Karpeev, Phys. Biol. **5**, 046003 (2008).
[49] B. M. Haines, A. Sokolov, I. S. Aranson, L. Berlyand, and D. A. Karpeev, Phys. Rev. E **80**, 041922 (2009).
[50] D. Saintillan, Exp. Mech. (to be published).
[51] E. J. Hinch and L. G. Leal, J. Fluid Mech. **52**, 683 (1972).
[52] E. J. Hinch and L. G. Leal, J. Fluid Mech. **76**, 187 (1976).
[53] H. Brenner and D. W. Condiff, J. Colloid Interface Sci. **47**, 199 (1974).
[54] H. Brenner, Int. J. Multiphase Flow **1**, 195 (1974).
[55] G. B. Jeffery, Proc. R. Soc. London, Ser. A **102**, 161 (1922).
[56] F. P. Bretherton, J. Fluid Mech. **14**, 284 (1962).
[57] G. K. Batchelor, J. Fluid Mech. **44**, 419 (1970).
[58] M. Wu, J. W. Roberts, S. Kim, D. L. Koch, and M. P. DeLisa, Appl. Environ. Microbiol. **72**, 4987 (2006).
[59] S. B. Chen and D. L. Koch, Phys. Fluids **8**, 2792 (1996).
[60] S. B. Chen and L. Jiang, Phys. Fluids **11**, 2878 (1999).
[61] R. Blanc, in *Mobile Particulate Systems*, edited by E. Guazzelli and L. Oger (Kluwer, Dordrecht, 1995).
[62] M. B. Mackaplow and E. S. G. Shaqfeh, J. Fluid Mech. **329**, 155 (1996).
[63] M. Abramowitz and I. A. Stegun, *Handbook of Mathematical Functions: With Formulas, Graphs, and Mathematical Tables* (Dover, New York, 1965).
[64] L. D. Landau and E. M. Lifshitz, *Fluid Mechanics* (Butterworth-Heinemann, Oxford, 1987).
[65] A. Alizadeh Pahlavan and D. Saintillan (unpublished).